

APPLICATION OF INSTRUMENTED INDENTATION TECHNIQUE TO ESTIMATE STRENGTH AND RESIDUAL STRESS

Min-Jae Choi^{1,}, Kyung-Woo Lee¹, Ju-Young Kim¹, Kwang-Ho Kim², and Dongil Kwon¹*

¹ *Department of Materials Science and Engineering, Seoul National University, Seoul, Korea*

² *Frontics Inc., Research Institute of Advanced Materials, Seoul National University, Seoul, Korea*

Abstract – The instrumented indentation technique has recently attracted significant research interest because of its various advantages such as nondestructive specimen preparation, easy process, and high spatial resolution. In particular, this technique is a promising alternative to measurement methods of tensile properties and residual stress. We can evaluate tensile properties and residual stress by analyzing the indentation load-depth curve. Tensile properties of materials, primarily yield strength and tensile strength, are obtained by defining representative stress and strain, through the numerous investigations of instrumented indentation curves, and the results were discussed by comparing with results of uniaxial tensile tests. Residual stress measurement technique is based on the key concepts that the deviatoric stress part of residual stress affects the change in indentation load-depth curve, and then by analyzing difference between residual stress-induced indentation curve and residual stress-free curve, quantitative residual stress of target region can be evaluated. In determining the stress-free curve of the target region, we take into consideration microstructural changes accommodating the strength difference. Micromechanical contact analyses for the residual-stress-induced load shifts yield stress values comparable to the applied in-plane stresses. This study supports the proposition that the surface stress in an arbitrary biaxial state can be evaluated through a theoretical model combined with the ratio of two principal stress components. Instrumented indentation tests and conventional tests were performed to verify the applicability of the suggested technique, and the estimated residual stress values obtained from the indentation technique showed good agreement with those from conventional tests.

Keywords : Instrumented Indentation Technique (IIT), Tensile Properties, Residual Stress

1. INTRODUCTION

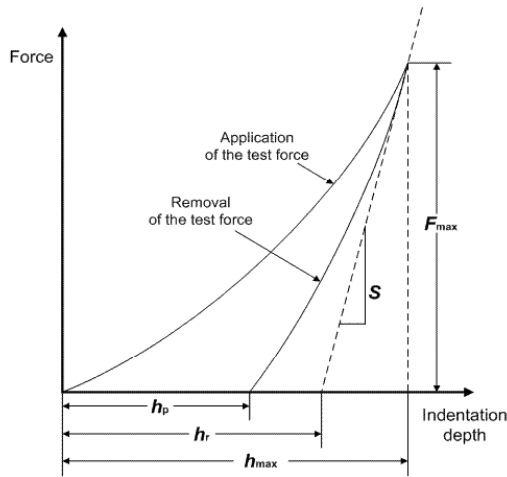
The frequent failure of structural components by time-dependent degradation in severe operating environments has recently become a concern. In particular, pipeline operating conditions are made more severe by cryogenic contents and many inhomogeneous welded joints, so that the welded joint is typically the initiation point of fracture because of the microstructural and mechanical inhomogeneities [1]. Thus

safety assessment based on precise mechanical properties of local regions is indispensable. However, conventional standard tests, such as uniaxial tensile tests need bulky standard samples and thus cannot be applied to in-service structures/facilities and local regions such as welded joints. Direct evaluation of weld mechanical properties is mainly limited to microhardness measurement, and indirect methods entail the testing of a bulky simulated specimen [2]. Thus a new mechanical testing method for locally welded joints is needed.

The residual stress resulting from welding is one of the most important factors in safety assessment. Welding thermal cycles generate inhomogeneous heating and cooling in the regions near the heat source, thus causing residual stress in the weldments that can exceed the yield strength of the welded material. It is well recognized that the presence of welding residual stresses is detrimental to weld performance. In particular, a region in tensile stress is susceptible to fatigue and stress-corrosion cracking [3]. Several techniques are used to measure or predict residual stress. Conventional measurement techniques can be divided into two groups: mechanical stress-relaxation methods and physical methods. Mechanical stress-relaxation methods, including hole-drilling and saw-cutting techniques, can generally be used to evaluate residual stress quantitatively without any reference sample, but they have limitations because they are destructive tests. Physical methods such as X-ray, neutron diffraction, magnetic Barkhausen noise and ultrasonic methods analyze residual stress nondestructively, but they always entail the considerable difficulty of separating microstructural effects on the physical parameters from those of residual stress, since all the techniques are highly sensitive to metallurgical factors such as grain size and texture [4]. Thus the results often show poor reproducibility and large scatter compared with mechanical methods. Similarly, it is almost impossible to use nondestructive methods to assess residual stresses in weldments including heat-affected zones (HAZs), which have very rapid microstructural gradients.

A nondestructive instrumented indentation technique has been developed [5,6] to overcome these limitations. This technique can evaluate various material/mechanical properties such as flow properties and residual stress by analysis of the indentation load-depth curve obtained during continuous indentation [7-10]. The tensile properties were

determined from the indentation load-depth curve continuously measured by a spherical indenter based on a representative stress and strain approach. By determining the precise contact depth and optimum representative stress and strain, tensile properties obtained from tensile tests and IIT were compared for 10 metallic materials. In addition, we adapt the residual stress model to a general biaxial stress state and use this model to characterize a friction stir-welded API X80 steel by suggesting proper assumptions for stress directionality and reference stress-free information. The residual stresses estimated are compared with those obtained by energy-dispersive X-ray diffraction.



(a)



(b)

Fig. 1. (a) Load-depth curve obtained from instrumented indentation test; (b) AIS (Advanced Indentation System) 3000, made by Frontics, Inc.

2. THEORITICAL MODEL FOR EVALUATING MECHANICAL PROPERTIES USING IIT

2.1 Flow Properties Measurement Using IIT

It is well known that the relationship of true stress and mean pressure P_m can be expressed as [6]

$$\sigma = \left(\frac{1}{\Psi} \right) P_m = \left(\frac{1}{\Psi} \right) \left(\frac{P}{\pi a_c^2} \right), \quad (1)$$

where Ψ is a plastic constraint factor, P is the load, and a_c is the contact radius. Most research on the indentation flow curve has used this definition of true stress. However, the plastic constraint factor has been regarded as a material-independent constant or as a function of the strain-hardening exponent. In this study, a constant value of 3.0 was used for the plastic constraint factor, as verified by finite element analysis (FEA) of various materials [15]. On the basis of the deformation shape and strain distribution under a spherical indenter, Ahn and Kwon proposed a new definition using the tangent function [9]. The displacement along the depth axis under the indenter, u_z , can be expressed geometrically as:

$$u_z = h - (R - \sqrt{R^2 - r^2}), \quad (2)$$

where R is the indenter radius and r is a radius at any point on the depth axis. The shear strain is derived by differentiating the displacement in the depth direction. The maximum shear strain is obtained at $r=a_c$, and Ahn and Kwon obtained the true strain by using a strain proportional constant:

$$\varepsilon = \left(\frac{\alpha}{\sqrt{1 - (a_c/R)^2}} \right) \left(\frac{a_c}{R} \right) = \alpha \tan \gamma, \quad (3)$$

where α was determined as 0.14 independent of material properties by FEA for various materials [15]. This definition covers a large range of true strain. The true stress and strain points obtained by IIT are fitted by a constitutive equation (Hollomon equation, $\sigma = K\varepsilon^n$), and K , a material constant, and n , the work-hardening exponent, are determined. Since the elastic modulus is obtained by IIT, the yield strength can be measured from the intersection point between the flow curve and a line with a slope of the elastic modulus 0.2% offset from origin. The ultimate tensile strain should be same as the strain-hardening exponent by the theory of instability in tension [16], and from this the tensile strength can be determined.

2.2 Residual Stress Evaluation Using IIT

A surface residual stress is assumed to be in an equibiaxial tensile state ($\sigma_{res,x} = \sigma_{res,y} = \sigma_{res}$, $\sigma_{res,z} = 0$) and uniform in the near-surface region (taken as about three times the indentation depth) [10,11]. If an arbitrary indentation state (h_i, L_0) is attained in an unstressed state and if the tensile in-plane stress σ_{res} is applied to the loading state at a fixed penetration depth h_i , the indentation load L_0 is reduced to a load L_T due to the decrease in surface penetration resistance. The load shift $L_T - L_0$ due to tensile stress is a clue for stress quantification. The surface-normal deviator stress σ_z^D is $-2\sigma_{res}/3$ by removing the hydrostatic stress $2\sigma_{res}/3$ from the surface residual stress σ_{res} and is added to the contact pressure [11]. $L_T - L_0$ is defined as a product of the selected deviator stress component and its corresponding contact area

A_C^T . Thus, an equation for the equibiaxial residual stress is derived in terms of the indentation load and contact area as:

$$\sigma_{res} = \frac{3(L_0 - L_T)}{2A_C^T} \quad (4)$$

Here A_C^T in the tensile stress state is calculated from $L_T A_C^0 / L_0$ because the contact hardness H or $L_0 / A_C^0 = L_T / A_C^T$ is independent of the elastic residual stress. In order to measure the actual contact area A_C^0 with pile-up or sink-in information from an Oliver-Pharr curve analysis [5], an empirical calibration for instrumental stiffness was performed by making preliminary indentation tests on API X80 steel [8].

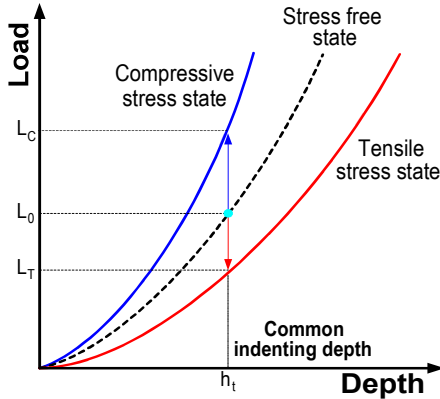


Fig. 2. Shift of indentation loading curve with changes in residual stress

Since the experiments and theoretical models described above treat only equibiaxial residual stress, the magnitude of the average stress effect can be determined through the instrumented indentation technique but the directionality and magnitude of an actual biaxial stress cannot. This impedes wide application of the instrumented indentation technique to complex biaxial stress states in actual structures [12]. If we denote one major stress component of the biaxial residual stress as $\sigma_{res,x}$ and the other as a minor stress component $\sigma_{res,y}$, $\sigma_{res,y}$ can be expressed as $p\sigma_{res,x}$ using the stress ratio p or $\sigma_{res,y}/\sigma_{res,x}$. The influence of biaxial stress on the indentation plasticity also can be analyzed through a similar hydrostatic-stress-removal method. The deformation-sensitive deviator stress component is given as $\sigma_z^D = -(1+p)\sigma_{res,x}/3$ in this case. Thus, if information on p is given, individual principal stresses can be calculated from the instrumented indentation test using (5). Note that (5) converges to (4) when the stress state approaches to the equibiaxial state or $p = 1.0$:

$$\sigma_{res,x} = \frac{3(L_0 - L_T)}{(1+p)A_C^T} \quad (5)$$

Lee and Kwon [8] showed the validity of (5) by empirical indentation tests on biaxially strained specimens. The stress ratio became an important issue in stress characterization, and Underwood's observation of a nonsymmetrical contact deformation in uniaxial stress [13]

supplied a clue to extracting the surface stress directionality. Lee et al. [14] tried to estimate the stress ratio by analyzing the pile-up heights along the two principal biaxial stress axes. The ratio of stress-induced pile-up shifts was linearly proportional to the stress ratio. Several preliminary observations on the welded joints yielded a stress ratio of about 0.33, and this value was used in subsequent biaxial stress analyses.

3. EXPERIMENTAL VERIFICATION OF THE MODELS

3.1 Measurements of Tensile Properties

10 steel materials were prepared and their surfaces polished with $1\mu\text{m}$ alumina powder. Indentation testing was performed using AIS 3000 equipment (Frontics Inc.) with load resolution of 5.6gf and depth resolution of $0.1\mu\text{m}$. The indenter was a WC ball of radius $250\mu\text{m}$ and the loading-unloading speed was $0.1\text{mm}/\text{min}$. The final maximum indentation was $150\mu\text{m}$ and 15 partial unloadings down to 50% maximum load at each point were performed.

TABLE I. Tensile properties obtained from tensile tests and instrumented indentation tests

Material	Yield strength [MPa]			Tensile strength [MPa]		
	Tensile	IIT	Error (%)	Tensile	IIT	Error (%)
P91	569.7	558.7	-1.9	772.0	807.5	4.6
S45C	372.9	336.4	-9.8	883.2	843.7	-4.5
SCM21	290.2	314.9	8.5	626.5	609.3	-2.8
SCM415	237.4	230.1	-3.1	616.3	620.7	0.7
SUJ2	306.8	270.2	-11.9	907.7	862.2	-5.0
SKD11	243.4	270.1	11.0	923.1	880.1	-4.7
SKD61	348.9	361.8	3.7	896.5	882.2	-1.6
SKS3	366.4	330.9	-9.7	781.5	810.6	3.7
API X65	451.8	522.9	15.7	610.8	630.3	3.2
API X70	592.9	550.9	-7.1	782.2	770.9	-1.4

To verify our analysis, the true stress and strain curves were measured by tensile tests at cross-head speed $1\text{mm}/\text{min}$ for specimens with gauge length 25mm and diameter 6mm . The tensile properties obtained from tensile tests and IITs are summarized in Table I and Fig. 3. The tensile strengths obtained by IIT were within $\pm 5\%$ of that from tensile tests. For yield strength, the error range was within $\pm 10\%$ except for some materials with high error value ($\geq \pm 10\%$). The first true stress-strain points were obtained with indentation depth $10\mu\text{m}$, which is about 4% representative strain if contact depth is calculated ignoring elastic deflection and pile-up/sink-in. Yielding happens at strains below 0.5% for

most metallic materials. The true stress-strain points with low strain value affect fitting of the constitutive equation more than the points with high strain value, since the Hollomon equation is a type of exponent function, which induces large deviation in yield strength relative to tensile strength. A possible reason for the high error in yield strength is the presence of Lüders strain, as shown in Fig. 3 (c), (d). If the length of Lüders strain is defined as ε_L , the yield strain ε_y can be estimated as

$$K\varepsilon_y^n = E(\varepsilon_y - 0.002 - \varepsilon_L). \quad (6)$$

For IIT, however, it is difficult to recognize and measure Lüders strain, and we leave this issue for future study.

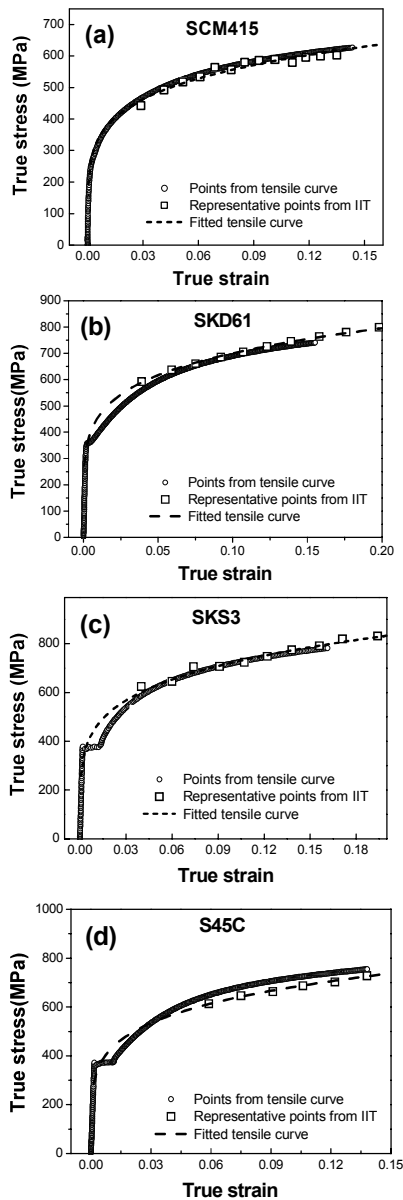


Fig. 3. Comparisons between tensile curves from uniaxial tensile tests and instrumented indentation tests for (a) SCM415, (b) SKD61 (without Lüders strain), (c) SKS3, and (d) S45C (with Lüders strain)

3.2 Experimental Evaluation of Residual Stress

3.2.1. Experimental procedures

API X80 steel of thickness 20mm was used in the friction stir-welding studies; its chemical composition (wt.%) was 0.13C, 1.52Mn, 0.26Si, 0.17Mo, 0.034Cr, 0.026Ni, 0.0002Nb, 0.003Ti, 0.062V, 0.041Al, 0.032Cu, 0.0003B. Test plates were sectioned in half along the rolling direction and prepared for a butt joint. Oxide scale was removed by sand grinding followed by degreasing with methanol. An argon gas atmosphere was used to prevent oxidation during the weld cycle. Friction stir welding was done with a polycrystalline cubic boron nitride tool in an inert gas environment (MegaStir Technology, UT, USA); tool rotation and travel speeds were 550rpm and $1.69\text{mm}\cdot\text{s}^{-1}$, respectively. Metallographic samples for optical observation, Vickers micro-hardness testing, instrumented indentation testing, and energy-dispersive X-ray diffraction (ED-XRD) observation were prepared from the welded joint using metallographic procedures followed by etching with 2% nital solution. Vickers micro-hardness was probed using a 0.1kgf load across the welded joint.

A commercial AIS 3000R (Frontics, Inc., Seoul, Korea) with depth and load resolutions of $0.1\mu\text{m}$ and 14.7mN was used for the instrumented indentation tests, which were performed across the friction stir-welded joint at 2mm intervals (a surface-parallel indentation-testing array was made 2mm from the welded surface). Two methods were used to obtain a reference indentation curve in a stress-free state corresponding to each microstructural region in the welds. The reference stress-free curve for the base metal, which underwent no microstructural change, was obtained directly from the remote base-metal region (about 10mm from the welds). In addition, a multiple-indentation method (5kgf load gap) was applied to characterize contact properties at several depth steps. The reference stress-free curve for the welding zone, which underwent significant microstructural change, was calculated through a unique analysis.

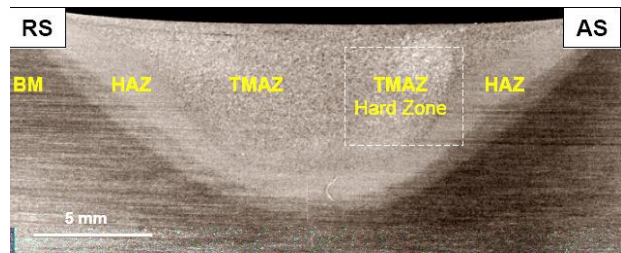


Fig. 4. Four distinctive microstructural regions within the friction stir-welded API X80

The maximum applied load and testing speed were 50kgf and 0.3mm/min. We used ED-XRD with a high-energy white-beam synchrotron radiation source. Profiling was done with the aid of highly collimated incident and scattered X-ray beams and with micro-positioning of the sample surface. The profiling depth can attain the order of mm, and can be controlled to within a few microns by radiation

energy. When obtaining strain measurements using ED-XRD, we focused the depth at about 200nm, similar to maximum indentation depth, to avoid any depth-difference effects between IIT and ED-XRD.

3.2.2. Residual stress distribution across the friction stir-welded joint

The instrumented indentation curves of the BM near the HAZ (solid triangles) and the reference curve for API X80 steel are presented together in Fig. 5. The load decrease due to surface stress at a given indentation depth means that the residual stress has positive sign (tensile). By inserting $p=0.33$ into (5), the quantitative stress distribution inside the base metal was calculated as plotted in Fig. 5. The BM reference indentation curve in Fig. 5 can be roughly fitted to $L=\alpha_B h^2$, where α_B is a hardness-proportional parameter (about upper 70% of the experimental solid line is fitted and overlapped in Fig. 5 as open triangles). The approximate reference indentation curves for the HAZ, TMAZ, and TMAZ-HZ also can be fitted by calculating corresponding α values. For example, α_{TMAZ} in the TMAZ is calculated from $\alpha_B H_{TMAX}/H_B$. The hardness ratio of the TMAZ and BM H_{TMAX}/H_B was about 1.21 and thus α_{TMAZ} was $7.76 \times 10^9 \text{ kgf} \cdot \text{m}^{-2}$ when α_B for the BM is given as $6.41 \times 10^9 \text{ kgf} \cdot \text{m}^{-2}$. Since the remnant indent morphologies from BM and other microstructures were very similar in this study, regardless of their different indent sizes, the values could be compared directly. If remnant indents from two materials for the comparison have no geometrical similarity (i.e., they have different convexity around the contact periphery), this geometrical discrepancy must be considered in determining the value to predict the proper shape of the loading curve.

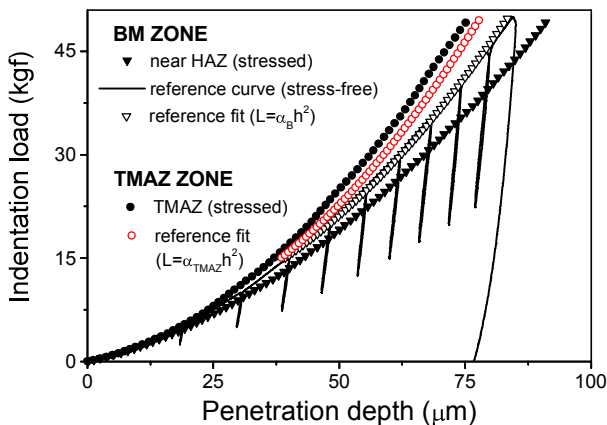


Fig. 5. Experimental indentation curves (solid triangles and circles) from welded joint in residual stress state and analytical reference curves (open triangles and circles) for stress-free state

The reference indentation curve calculated for the TMAZ-HZ is also plotted in Fig. 5 as open circles. Superposing the stressed indentation data and the newly calculated reference stress-free curve of the TMAZ (solid and open circles in Fig. 5) makes it possible to calculate a quantitative stress distribution in the TMAZ region. The

stress distributions in the HAZ and TMAZ-HZ were also estimated by similar procedures. Finally, the whole stress distribution of the friction stir-welded joint is plotted in Fig. 6 (solid circles). The residual stress profile measured from ED-XRD is also plotted in Fig. 6 (open circles).

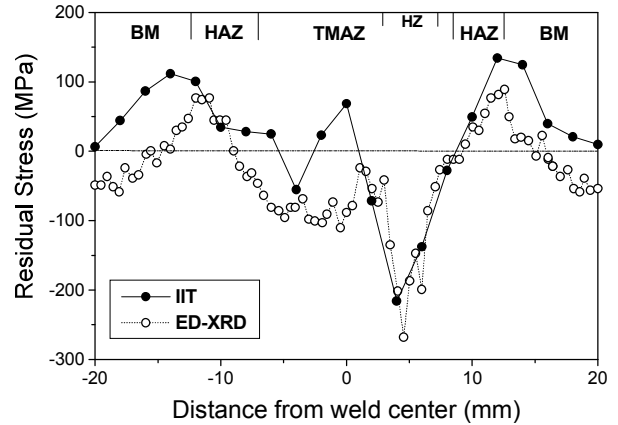


Fig. 6. Residual stress distributions measured from the instrumented indentation technique (IIT) and energy-dispersive X-ray diffraction (ED-XRD)

Except for the slight negative shift of the ED-XRD results (less than 50MPa), the residual stress distributions from the IIT and ED-XRD were consistent throughout the whole welded joint. The discrepancy can be attributed to the indirectly calculated reference indentation curve and approximately determined stress ratio. The maximum tensile residual stress, about 150MPa, was estimated near the BM-HAZ boundary, meaning that the BM-HAZ boundary is vulnerable to external loads. In addition, the high microhardness in the TMAZ-HZ region can be partly explained by the high compressive stress caused by the complex thermal cycle and phase transformation during friction stir welding. These experimental results suggest that the instrumented indentation technique is a promising nondestructive stress-measurement technique, especially for welded joints. However, the sparse indentation results, i.e. the 2-mm gap preventing the deformation field overlap, must be improved for more local welds by adopting such indentation techniques as zigzag probing.

4. CONCLUSION

The residual stress profile assessed from the instrumented indentation tests showed high tensile stress (or compressive stress) near the base metal and heat-affected zone boundary (or near the thermo-mechanically affected zone-hard zone). Although there was a slight difference in quantitative value, the stress trend in instrumented indentation testing was completely consistent with the energy-dispersive X-ray diffraction results. Tensile properties of 10 metallic materials were obtained using IIT by applying the representative stress and strain approach. Comparison of tensile properties from IITs with those from uniaxial tensile tests yielded an error range in the tensile strength of $\pm 5\%$. For yield strength, the error range was $\pm 10\%$ except for

some materials with high error value ($>\pm 10\%$). The larger error range is basically due to the mathematical form of Hollomon equation, and the presence of Lüders strain may have affected the yield strength.

REFERENCES

- [1] B. C. Kim, "Microstructure and Local Brittle Zone Phenomena on High-Strength Low-Alloy Steel Welds", *Metall. Mater. Trans. A*, vol. 22, pp. 139-149, 1991.
- [2] D. Rosenthal, "The Theory of Moving Sources of Heat and Its Application to Metal Treatments", *Transaction of ASME* vol. 68, pp. 849-860, 1946.
- [3] I. C. Noyan, J. B. Cohen, "Residual Stresses", *Springer-Verlag*, New York, 1987.
- [4] Society for Experimental Mechanics, Inc. (edited by J. Lu), "Handbook of Measurement of Residual Stresses", *Fairmont Press*, Lilburn, GA, 1996.
- [5] W. C. Oliver, G. M. Pharr, "An Improved Technique for Determining Hardness and Elastic Modulus Using Load and Displacement Sensing Indentation Experiments", *J. Mater. Res.*, vol. 7, pp. 1564-1583, 1992.
- [6] D. Tabor, "Hardness of Metals", *Clarendon Press*, UK, 1951.
- [7] J. Y. Kim, K. W. Lee, J. S. Lee, D. Kwon, "Determination of Tensile Properties by Instrumented Indentation Technique: Representative Stress and Strain Approach", *Surf. Coat. Technol.*, vol. 201, pp. 4278-4283, 2006.
- [8] Y. H. Lee, D. Kwon, "Estimation of Biaxial Surface Stress by Instrumented Indentation with Sharp Indenters", *Acta Mater.*, vol. 52, pp. 1555-1563, 2004.
- [9] J. H. Ahn, D. Kwon, "Derivation of Plastic Stress-Strain Relationship from Ball Indentations: Examination of Strain Definition and Pileup Effect", *J. Mater. Res.*, vol. 16, pp. 3170-3178, 2001.
- [10] Y. H. Lee, D. Kwon, "Measurement of Residual Stress Effect by Nanoindentation on Elastically Strained (100 W)", *Scripta Mater.*, vol. 49, p. 459, 2003.
- [11] S. Suresh, A. E. Giannakopoulos, "A New Method for Estimating Residual Stresses by Instrumented Sharp Indentation", *Acta Mater.*, vol. 46, p. 5755, 1998.
- [12] A. E. Giannakopoulos, "The Influence of Initial Elastic Surface Stresses on Instrumented Sharp Indentation", *J. Appl. Mech.*, vol. 70, pp. 638-643, 2003.
- [13] J. H. Underwood, "Residual-stress measurement using surface displacements around an indentation", *Exp. Mech.*, vol. 13, pp. 373-380, 1973.
- [14] Y. H. Lee, K. Takashima, Y. Higo, D. Kwon, "Prediction of Stress Directionality from Pile-up Morphology Around Remnant Indentation", *Scripta Mater.*, vol. 51, pp. 887-891, 2004.
- [15] E. Jeon, M. K. Baik, S. H. Kim, B. W. Lee, D. Kwon, "Determining Representative Stress and Representative Strain in Deriving Indentation Flow Curves Based on Finite Element Analysis", *Key Eng. Mater.*, vol. 297-300, pp. 2152-2157, 2005.
- [16] G. E. Dieter, "Mechanical Metallurgy", *McGraw-Hill*, Hightstown, NJ, 1986.

Author: Min-Jae Choi

Address: 30-319, Department of Materials Science & Engineering,
Seoul National University, Kwanak-gu, Seoul, Korea, 151-742

Tel : +82-2-880-8025; Fax : +82-2-886-4847

E-mail: mjtakel@snu.ac.kr